A REVIEW OF PROPELLER THEORY

By Blake W. Corson, Jr.

Langley Aeronautical Laboratory

INTRODUCTION

Although the use of screw propellers for boats was introduced at least as early as 1836, the scientific study of propellers may be regarded as having begun in 1865 with the introduction of the slipstream-momentum theory by Rankine which was followed in 1878 by an alternative concept, the simple blade-element theory of W. Froude. In view of the extreme simplicity of the assumptions upon which the early theory is based, the agreement of the analytical results with experience is remarkably good. The fact that no further major advances in propeller theory were made until about 1915 is due in part to the relatively satisfactory results obtained with the early simple theory and indicates that progress in propeller theory awaited the development of aircraft and airfoil theory.

In the history of propeller theory there appear to be five outstanding contributions which serve as a background for a great number of associated significant contributions. The major contributions are the axial-momentum theory introduced by Rankine (reference 1) in 1865, the simple blade-element theory of W. Froude (reference 2), 1878, the concept of the vortex propeller theory by Lanchester (reference 3), 1907, the screw propeller with minimum induced energy loss by Betz (reference 4), 1919, and Goldstein's solution for the radial distribution of circulation for highest efficiency for a lightly loaded propeller having a finite number of blades (reference 5), 1929. Since 1929 a number of notable contributions have been made to aerodynamic propeller theory, most of which stem from an attempt to extend the work of Betz and Goldstein to consideration of a heavily loaded propeller and the development of dual-rotation propeller theory.

A review of only the significant contributions to propeller theory affords material for a voluminous textbook. The purpose of this paper is to mention briefly the significant features of the major contributions and to discuss some of the more important developments made since the introduction of Goldstein's work, especially those made during the recent war years which have not received widespread publicity.

A list of the symbols used in this paper is included in the appendix.

EARLY THEORY

Simple Momentum Theory

In the development of the slipstream-axial-momentum theory Rankine regarded the propeller as an actuator disk immersed in a fluid having a uniform relative motion normal to the plane of the disk as shown in figure 1. The thrust exerted by the propeller results in a discontinuous increase in total pressure of the slipstream as it passes through the disk which is manifest as a continuous increase in slipstream axial velocity and an abrupt rise in static pressure. In the derivation, use is made of the laws of motion, Bernoulli's equation, continuity equation, and conservation of energy. The analysis indicates that the axial-velocity increase in the fully developed slipstream, where the static pressure is the same as that of the surrounding medium, is twice the increase at the propeller. The fundamental and very useful relation for jet propulsive efficiency is

$$\eta = \frac{1}{1 + a} \tag{1}$$

By assuming conservation of energy, an alternate expression involving power coefficient, advance ratio, and efficiency is derived:

$$C_p = \frac{\pi}{2} J^3 \frac{\eta - 1}{\eta^3} \tag{2}$$

Equation (2) represents the absolute ultimate in efficiency obtainable with a loaded propeller operating in an undisturbed stream; the only loss considered is the axial kinetic energy in the slipstream which is inseparable from the production of thrust. The variation of ideal efficiency with advance ratio as indicated by the simple momentum theory is shown in figure 2 and is compared with the efficiency indicated by modern theory.

The simple momentum theory was inadequate in that it gave no indication of the rate of slipstream contraction, failed to deal with the friction losses of a real propeller, and failed to fix propeller geometry except to demand the largest possible diameter.

Simple Blade-Element Theory

The simple blade-element theory introduced by W. Froude in 1878 and extended by Drzewiecki (reference 1 on p. 179 of reference 6) in 1892 ignored the concept of slipstream momentum and considered only the

force and velocity vectors acting on the propeller blade sections. The blade section at each radial distance from the axis of rotation was treated as an airfoil of indefinitely short span operating in a fluid whose relative velocity was determined only by the propeller's rotational speed and its forward motion. Application of the theory required the use of experimentally determined airfoil characteristics (lift and drag coefficients) and arbitrary assumptions of effective aspect ratio.

This theory, though far from being satisfactory, did enable designers to fix propeller size and shape for given operating conditions and permitted the calculation of propeller thrust, power, and profile efficiency. The efficiency computation accounts for no losses except the blade-section profile-drag or friction losses. The efficiency of a blade element η' is expressed as

$$\eta' = \frac{\tan \phi_o}{\tan \left(\phi_o + \gamma \right)} \tag{3}$$

where ϕ_o is the nominal helix angle and γ is the angle whose tangent is the drag-lift ratio. The foregoing relation is simply the efficiency of any screw involving friction and working without slip. The theory is useless for conditions of low rates of advance but gives reasonably good results at high advance ratios and does indicate that highest efficiency can be obtained when the most effective parts of the propeller blade have helix angles slightly less than 45°. Inasmuch as the energy relations between the propeller and the surrounding medium are ignored, the theory is incomplete and gives no information for selection of optimum number of blades or optimum blade shape. The optimum diameter indicated would be merely that which resulted in lowest profile losses which is entirely dependent upon the arbitrary selection of airfoil characteristics.

MODERN THEORY

The Vortex Theory

In the quarter century preceding World War I, considerable effort was spent in trying to develop the older basic theories to have a more realistic application to actual propellers. Most investigators realized that the axial-velocity increment demanded by the simple momentum theory must also exist to some extent for the blade-element theory, and early attempts to improve the latter theory followed this approach. That is, the effective axial velocity in which the propeller operated was assumed to be the sum of the flight velocity and the velocity increment (at the disk) calculated from the simple momentum theory or an empirically determined portion thereof (reference 1 on p. 180 of reference 6 and references 7 and 8). Also, during this period the slipstream-momentum

theory was extended to include the slipstream rotation resulting from propeller torque and was designated as the general momentum theory.

With the advent of modern airfoil theory characterized by the association of lift with circulation and the related concept of a vortex system for a finite airfoil consisting of bound and trailing vortices, a new approach to the propeller problem was opened.

The concept proposed by Lanchester in 1907 (reference 3), upon which the vortex theory of the propeller is based, is that the effective velocity at which the blade sections of a propeller operate includes, in addition to the translational and rotational velocities, the velocity induced by the propeller itself which is the strength at the propeller blades of the velocity field of the trailing vortex system. This concept is based on Prandtl's airfoil theory. The simplest possible representation of such a system, analogous to the use of a horseshoe vortex to represent a finite lifting airfoil, is shown in figure 3. The diagram illustrates the propeller blades, each with a bound vortex and its associated pair of trailing vortices, all of equal strength. From each propeller blade one vortex trails directly downstream with circulation about the axis of rotation in the same sense as the propeller rotation, the other vortex springing from the propeller tip trails along a helical path with circulation opposite in sense to that of the axial trailing vortex. It was realized, of course, that the real vortex system would be determined by the radial distribution of load on the blade and would be composed of a helicoidal sheet of vortex filaments springing from all points along the blade. Employing such a concept, Joukowski developed a vortex theory of screw propellers in 1912 (reference 8 on p. 180 of reference 6) which he presented in final form in 1918, being forced by the involved nature of the problem to the simplifying assumption of an infinite number of blades. Original contributions in the development of the vortex theory of propellers with an infinite number of blades have been made by other investigators (references A5 and A7 of reference 9 and references 10 to 13) of whom the most widely known in English speaking countries is H. Glauert.

The essential feature of the vortex theory is that the induced velocity at the propeller blade can be calculated from a knowledge of the vortex system of the wake and that in the resultant flow the blade elements can be assumed to operate with the characteristics of an airfoil having infinite aspect ratio. A further assumption made in the application of blade-element theory is that the operation of a blade element is not influenced by the operation of adjacent elements of the same blade. Though not theoretically tenable, experiment has shown that the assumption of independence of blade elements results in no appreciable error (reference 14).

A typical vector diagram of the velocities assumed to act on a propeller blade element for the vortex theory is presented in figure 4. The axial and rotational components, v and $2\pi rn$, respectively, are

specified by the operating conditions. The critical problem in any screw-propeller theory is the determination of the induced velocity w_1 which is the real velocity at the propeller blade element of the air adjacent to the vortex sheet in a direction normal to the sheet. In the application of the vortex theory it has been customary to resolve the induced velocity into axial and rotational components and to compute these "interference" velocities by means of the general momentum equations. Satisfactory routing procedures for application of the vortex theory have been set up by Glauert and by Weick (references 15 and 16, respectively).

Again referring to the vector diagram (fig. 4) the efficiency of a blade element by the vortex theory is shown to be

$$\eta' = \frac{\tan \phi}{\tan (\phi + \gamma)} \frac{1 - a'}{1 + a} \tag{4}$$

Equation (4) conveniently indicates the magnitudes of the three sources of loss considered, that is, profile-drag loss and the axial and rotational induced losses.

When the vortex theory is simplified by the assumption of a propeller having an infinite number of frictionless blades, the induced velocity at the propeller w_1 of the trailing-vortex system is the same as that obtained by the general momentum equations and is given by

$$w_1 = \frac{B\Gamma}{4\pi r \sin \phi} \tag{5}$$

where the product $B\Gamma$ is the total circulation about all blade elements at the radius r.

In spite of the necessary simplifying assumptions, the vortex theory has given results which agree reasonably well with experience and forms the basis of modern propeller theory. It did fail, however, in the important detail of showing the effect of the number of blades and, as originally developed, did not indicate the optimum radial distribution of blade loading.

Screw Propeller with Minimum Induced Energy Loss

Adopting the concept of a propeller operating in accordance with the vortex theory and producing a slipstream composed of a system of trailing vortices, Betz proposed to determine the radial distribution of circulation along the propeller blade (or distribution of vorticity in

the slipstream) which for a given thrust would result in the smallest energy loss (reference 4). Prandtl had shown that the condition of minimum induced energy loss for a lifting airfoil is obtained when the induced velocity in the wake, opposed to the direction of the lift, is uniform along the span, which results in an elliptical spanwise loading. Betz's solution represents an extension of Prandtl's airfoil theory to the case of a propeller. Just as in the case of a finite wing, the system of vortex filaments trailing the spanwise wing elements is regarded as forming a rigid sheet; so, for a propeller the vortex filaments trailing along helical paths downstream from the propeller blade elements are regarded as forming, behind each blade, a rigid helicoidal vortex sheet (without any assumption at this point as to whether the individual filaments continue to maintain their positions relative to one another as they pass downstream).

In the wake of a thrusting propeller the helicoidal sheets have both axial and rotational velocity components which, if the sheets are rigid, can be resolved into a pure apparent axial motion or pure apparent rotation. In any case the fluid between adjacent sheets adopts the same general motion and, in addition, a radial velocity produced by its tendency to flow around the edges of the sheets which produces the so-called "tip loss" associated with a finite number of blades. In his early treatment Betz assumed a lightly loaded propeller with negligible slipstream contraction. He dealt with conditions in the wake far behind the propeller and made use of Munk's displacement theorem by which a small change in circulation can be assumed to be added at a point in the wake rather than at the propeller blade.

Betz assumed that the radial distribution of circulation could be varied at will by adding or subtracting increments of circulation at various radii. He showed that to maintain a constant value of over-all thrust an increment of circulation removed at one radius had to be replaced at another by an increment having a strength inversely proportional to the respective radii. He then investigated the possibility of reducing the circulation at those radii where the induced loss was high and increasing the circulation at radii where the induced loss was small and thereby established the condition of minimum induced energy loss to be that for which the helicoidal vortex sheets formed apparently rigid screw surfaces of uniform pitch, under which conditions the blade elements at all radii operated with equal efficiency (drag losses not being considered).

Betz used rigorous proofs to establish the condition for minimum induced energy loss for a screw propeller, to justify the use of Munk's displacement theorem, and to show that the induced velocities in the fully developed slipstream were twice as great as for corresponding points at the propeller blades.

The condition for minimum induced energy loss is illustrated by the vector diagrams of figure 5 for velocities in the wake far downstream from the propeller. Betz's conclusion was that the induced velocity w_1

normal to the local surface of the vortex sheet should vary radially so that

$$\frac{w_1}{\cos \phi} = w = \text{Constant}$$

where w is the apparent axial motion of the rigid vortex sheets. The real velocity w_1 of the air at the surface of the helicoidal sheet has both axial and rotational components which vary continuously along the blade. However, to an observer far to one side of the slipstream viewing the wake system in a direction normal to its axis, the vortex sheets would appear to form rigid screw surfaces of uniform pitch and would appear to move as a whole without rotation with the pure axial velocity w.

The foregoing concept of a rigid-wake system is adopted for convenience in the mathematical treatment of the potential flow in the propeller wake. Because the induced velocities in the far wake are twice as great as at the propeller, the helicoidal vortex sheets undergo an initial distortion in the region where the slipstream contracts and are assumed then to form rigid screw surfaces of infinite length. Actually, the surfaces roll up into concentrated spiral vortices, one for each blade, and a single vortex along the axis equal to the combined strength of the spiral vortices.

In the development of propeller theory various authors deal sometimes with conditions at the propeller blades and at other times with those in the fully developed slipstream. In nearly all modern treatments of the vortex theory conditions in the final wake (especially, the apparent axial motion of the trailing helicoidal sheets) are the design criterions. It is the responsibility of the individual to make certain of an author's nomenclature before applying his results. The symbol w is found in the literature to represent axial velocity of the helices both in the final wake and at the propeller blades.

Effect of Number of Blades

In the development of the vortex theory the treatment of the propeller was simplified by the assumption of an infinite number of blades. In this way the spacing between adjacent helicoidal vortex sheets is made indefinitely small, the radial velocity components of the flow around the edges of the vortex sheets are eliminated from the considerations, and the circulation in a bound vortex does not become zero at the blade tip. For physical propellers the foregoing simplification must be abandoned; the spacing between the helicoidal sheets increases as a function of advance ratio and inversely as the number of blades; and further, the circulation in a bound vortex must become zero at the blade tip as well as at the axis. However, the Betz condition for

minimum induced energy loss that the helicoidal vortex sheets form screw surfaces of uniform pitch remains valid.

Prandtl's solution.- In an addendum to Betz's paper (reference 4), Prandtl gave an approximate solution for the radial distribution of circulation for a propeller having few blades. Prandtl ignored the helical nature of the flow behind a propeller and assumed the helicoidal vortex sheets to be replaced by a succession of semi-infinite, rigid-plane laminae normal to the propeller axis. The distance between laminae was taken equal to the normal distance at the slipstream boundary between the corresponding helicoidal surfaces, and the edges of the laminae were taken to lie in a plane tangent to the slipstream boundary. Prandtl investigated the two-dimensional field of flow around the edges of the laminae when the ambient fluid moved normal to their planes with a relative velocity w. Regarding the circulation as equal to the change in the velocity potential across the laminae, Prandtl obtained a distribution of circulation which was zero at the edge and increased with distance from the edge. The results applied to a propeller give a radial distribution of circulation which is a function of number of blades and advance ratio and is zero at the blade tip. When equations presented in reference 17 are combined, the approximate solution for optimum distribution of circulation along the blade obtained by Prandtl is given by equation (6) in terms of the circulation function

$$K(x) = \frac{B\Gamma_n}{Vw} = \frac{x^2}{1 + x^2}\frac{2}{\pi}\arccos e^{-\left[\frac{B}{2}(1-x)\sqrt{\left(\frac{\pi}{J}\right)^2+1}\right]} \qquad (6)$$

When Goldstein's exact solution (discussed subsequently) is used as a criterion, Prandtl's approximate solution gives good results for propellers having a large number of blades or having a small advance ratio, that is, when the spacing between adjacent helicoidal sheets is relatively small. For operation at large values of advance ratio, or with few blades, the approximate solution is not accurate. In all cases the approximate solution gives values of circulation larger than those obtained by Goldstein's exact solution.

Goldstein's solution.- An exact solution for the radial distribution of circulation in the helical wake of a propeller having few blades was obtained by Goldstein and presented in 1929 (reference 5). Lock (reference 18) states that the problem of pure hydrodynamics considered by Goldstein is that of the potential flow of fluid past a rigid body of a certain form moving with a uniform velocity. The form of the body is a helicoidal surface of infinite length but finite radius, moving parallel to its axis with uniform velocity w, or more generally any finite number of such surfaces equally spaced on the same axis and of the same radius, corresponding in number to the number of blades of the airscrew.

Goldstein deals with a propeller having few blades operating in an inviscid fluid so that the consideration of blade drag loss is eliminated. He accepts as valid the Betz condition for minimum energy loss as being realized when, at a great distance from the propeller, the vortex sheets trailing the propeller blades form screw surfaces of uniform pitch. Goldstein notes that acceptance of the foregoing condition is equivalent to neglecting the slipstream contraction and is therefore valid only for lightly loaded propellers. In obtaining his solution Goldstein deals only with conditions in the final wake and states, as does Betz, that the induced velocity at a propeller blade is one-half as great as that at a corresponding point in the wake.

In a few brief steps Goldstein establishes the differential equation for the potential flow which satisfies the boundary conditions. However, the mathematical procedures used to obtain a solution are intricate. The solution is obtained in terms of a circulation function $K(x)$

$$K(x) \equiv \frac{B\Gamma n}{Vw} = f(B, \phi, x)$$

The determination of the value of $K(x)$ for a specific operating condition involves the use of Bessel functions and the evaluation of infinite series.

A diagram of a propeller with its trailing vortex system is presented in figure 6 to illustrate the definition of the circulation function $K(x)$. This figure was taken in part from one presented in reference 19. A four-blade propeller operating at a flight speed V and rotational tip speed πnD is represented. On the lower blade in the figure the bound vorticity is represented by equipotential lines which, when shed, continue downstream as trailing-vortex filaments, the aggregate of which build the helicoidal vortex sheets. Goldstein assumed a lightly loaded propeller with negligible slipstream contraction so that at the surface of a vortex sheet in the far wake the circulation at a given radius could be equated to the circulation about the propeller blade at the same radius. The circulation Γ at a point on a vortex sheet is equivalent to the difference in the velocity potential between the upstream and downstream faces of the sheet taken along a path around the edge of the sheet.

By hypothesis the wake vortex system conforms to the Betz condition for minimum energy loss and moves axially with velocity w with respect to the surrounding medium. The axial spacing between adjacent helicoidal sheets is

$$\frac{V + w}{Bn}$$

The quantity

$$\left(\frac{V + w}{Bn}\right)w$$

represents the equivalent velocity potential resulting from the action of the velocity w through the axial distance between adjacent sheets. The circulation function $K(x)$ is defined as the ratio of the circulation Γ to this velocity potential:

$$K(x) = \frac{\Gamma}{\left(\frac{V + w}{Bn}\right)w}$$

$$= \frac{B\Gamma n}{(V + w)w}$$

The helix angle in the far wake is determined by the relation

$$\tan \phi = \frac{V + w}{2\pi rn}$$

In defining the circulation function for lightly loaded propellers, Goldstein regarded the wake velocity w as small compared to the flight speed so that

$$K(x) = \frac{B\Gamma n}{Vw}$$

For propellers with a moderately heavy loading he notes that it is more exact to define

$$K(x) = \frac{B\Gamma n}{(V + w)w}$$

One concept of the circulation function $K(x)$ is that it represents the fraction of the axial spacing between surfaces which, if acted through by the constant velocity w, produces the same potential as does the average of the real axial-velocity component acting through the full distance of the axial spacing. In other words, $K(x)w$ is the average value of the axial component of the induced velocity at a given radius.

In the simple case of a propeller with an infinite number of blades this is easily visualized. The helicoidal surfaces are indefinitely closely spaced; there is no radial flow; and the average axial induced velocity is the same as at the helicoidal surface and is $w \cos^2 \phi$:

$$K(x)w = w \cos^2 \phi$$

$$= \frac{B\Gamma}{\frac{V + w}{n}}$$

The total circulation $B\Gamma$ at a given radius is equivalent to the velocity potential produced by the average axial induced velocity acting through the axial distance traversed in one turn.

In figure 6 a qualitative representation of the streamlines referred to axes fixed in the surrounding fluid is shown on a plane approximately normal to the helicoidal sheets at their edges. The component of air velocity normal to a helicoidal sheet at any radius is the same on both faces of the sheet. The radial component of the velocity, however, is different, being directed inward at the upstream face and outward at the downstream face as a result of the tendency of the air to flow around the edge of the sheet. This discontinuity of the radial velocity at opposite faces of the helicoidal surface is a measure of the vortex strength or circulation. The energy of the radial flow accounts for the so-called "tip loss."

Goldstein presents values of the circulation function for a two-blade propeller plotted as a function of the cotangent of the helix angle with π/J as a parameter. He compares the values obtained by his exact solution with those obtained from Prandtl's approximate solution. Goldstein's results are shown in figure 7.

A comparison of the radial distribution of load for the simple momentum theory, the vortex theory ($B = \infty$), and Goldstein theory is presented in figure 8. In each case the propeller operates at an advance ratio of 2.0 and a power coefficient of 0.2. The comparison is of the thrust-grading curves. For the simple momentum theory this curve is a straight line through the origin corresponding to a uniform pressure rise across the disk. For the vortex theory for an infinite number of blades there is no tip loss, and thrust is assumed to be maintained at the blade tips. The curve for the Goldstein theory illustrates that the circulation must drop to zero at the tip. The table in the figure indicates the values of apparent axial velocity of the vortex system resulting in each case, as well as the respective values of efficiency.

Lock.- Prior to Goldstein's work on propeller theory, the vortex theory for an infinite number of blades had come into widespread use, and propeller investigators were familiar with the somewhat standardized form of equations by which the vortex theory was applied. Lock and Yeatman, in reference 20, show that the insertion of a factor κ into the standard equations for the vortex theory made these equations applicable to propellers having a finite number of blades where

$$\kappa = \frac{K(x)}{\cos^2\phi}$$

The circulation function $K(x)$ is defined by Goldstein for moderately loaded propellers as

$$K(x) = \frac{B\Gamma h}{(V + w)w}$$

For the vortex theory for infinite number of blades the circulation function so defined is found to be

$$K(x) = \frac{B\Gamma h}{(V + w)w}$$

$$= \cos^2\phi$$

Hence, for an infinite number of blades the function κ defined by Lock is unity:

$$\kappa = \frac{K(x)}{\cos^2\phi} = 1.0$$

The critical velocity component in propeller-blade-element theory is the induced velocity w_1 at the propeller blade normal to the resultant velocity. For the vortex theory for infinite number of blades this induced velocity, where $B\Gamma$ is the total circulation around the disk at radius r, is

$$w_1 = \frac{B\Gamma}{4\pi r \sin\phi}$$

Lock shows that the equivalent expression for the vortex theory with Goldstein's correction for a finite number of blades is

$$w_1 = \frac{B\Gamma}{4\pi r \kappa \sin \phi}$$

Values of κ lie, in general, between zero and unity. When the number of blades approaches infinity, Goldstein's $K(x)$ approaches $\cos^2\phi$ and κ approaches unity. Lock and Yeatman have extended the computation of Goldstein's $K(x)$ to cases for propellers having two, three, and four blades and have presented the results in charts showing κ as a function of $\sin \phi$ with the radius as a parameter (reference 20). A sample chart is shown in figure 9.

Crigler and Talkin (reference 21) present charts of $K(x)/\cos^2\phi$ for propellers having two, three, four, six, and eight blades. For such propellers they also give very useful charts of ideal efficiency (blade-section drag neglected) as a function of power coefficient, with blade loading σc_l at $x = 0.7$ and advance ratio as parameters, and show how these charts may be used to estimate quickly the over-all efficiency, thrust coefficient, and power coefficient, including the effects of drag.

Effect of Blade Profile Drag

In the development of propeller theory the potential-flow problem is usually set up for idealized conditions. The flow field of the propeller is regarded as being established by the flight speed, propeller rotational speed, and the velocities induced by the vortex system. The propeller blades are replaced by bound vortices of the desired strength, and the physical shape of a blade is ignored. The effects of the blade section drag on potential flow are regarded as of second order and are neglected. This is a logical procedure for establishing optimum ideal blade loading and the associated induced flow field.

In the application of theory to design the blade section drag must be considered because a large portion of the energy loss for a propeller is that due to profile drag. Lock (reference 22) makes a direct computation of the profile-drag power loss as being, for each blade element, the product of section drag and resultant velocity, which, when integrated, gives the loss for the entire propeller. Weick (reference 16) bases propeller drag loss on the section drag-lift ratio,

$$\eta_o' = \frac{\tan \phi}{\tan (\phi + \gamma)}$$

where

$$\tan \gamma = \frac{c_d}{c_l}$$

He shows that highest elemental efficiency is obtained when

$$\phi = 45^\circ - \frac{\gamma}{2}$$

and, consequently, that from consideration of only drag, a propeller of highest efficiency should be designed for an advance ratio slightly less than 2.20 which corresponds to a helix angle of 45° at $x = 0.7$.

In a study of the induced flow field of propellers of highest efficiency having a finite number of blades, Ferri (reference 23) considers the effect of blade section drag upon the ideal radial distribution of circulation. He shows that as the drag-lift ratio is increased an inboard shift of the blade loading is required to maintain highest over-all efficiency.

Hartman and Feldman (reference 24), basing their work on that of Goldstein and Lock, offer a systematic procedure for the design of propellers of highest efficiency including the effect of blade-section profile drag. They investigate the relation between the induced loss and drag loss for a propeller and show that when a specific propeller operates at its highest efficiency the drag loss is equal to the induced loss. Their treatment of the propeller is analogous to that which, for a finite wing, shows the maximum lift-drag ratio to be obtained when the induced drag equals the profile drag. Although their analysis is not rigorous, the conclusion is apparently substantiated by experiment. In figure 10 the envelope efficiency and corresponding values of power coefficient plotted against advance ratio are shown as solid-line curves. These data, from reference 25, were obtained in the Langley propeller-research tunnel for a 10-foot-diameter three-blade propeller, designated as 5868-9, with spinner. For identical values of power coefficient and advance ratio, the ideal efficiency of a three-blade propeller is shown as a dash line. At the advance ratio for maximum efficiency the induced loss is found to be very nearly equal to the drag loss. Similar computations for a number of different propellers have yielded like results. This type of analysis provides one means of judging the excellence of a propeller design. Also, in selection of diameter, when the propeller geometrical shape and operating conditions are fixed, the optimum diameter is that which results in equal induced and profile-drag losses.

The systematic design procedure offered by Hartman and Feldman is most readily applied when the NACA 16-series airfoil sections

(reference 26) are used. These sections which were developed especially for application to propellers have very high critical speeds and, at present, are the blade sections most widely used in the design of high-speed propellers.

Dual-Rotation Propellers

The history of dual-rotation propellers in the inventional stage begins almost as early as that for single-rotation propellers, but the development of fundamental theory for dual propellers has not progressed to a comparable stage. No rigorous proof for the optimum wake configuration comparable to Betz's treatment for single-rotation propellers has been established, nor has a mathematical solution for the distribution of the circulation along the blade been obtained. A large amount of literature exists which deals with the practical phases of dual rotation. An approximate design procedure, proposed by Lock, based essentially on single-rotation-propeller theory is presented in reference 27. A consideration of the periodic effects in dual-rotation propellers is treated in reference 28. A treatment of dual-rotation-propeller theory and design believed to be basically sound, but dependent upon an experimental approach, has been presented by Theodorsen (references 29 to 33). A simplified design procedure for dual propellers based upon Theodorsen's work has been presented by Crigler (reference 34).

The principal contributions to propeller theory made by Theodorsen are (1) the demonstration that the circulation function for any propeller could be determined by an electrical analogy with relatively simple apparatus and (2) the experimental determination of the circulation function for dual-rotation propellers, a problem which presents formidable difficulties to the mathematical approach.

Circulation function.- In dealing with single-rotation propellers having a finite number of blades, both Prandtl and Goldstein solved for the radial distribution of circulation along the propeller blade which they expressed as a nondimensional ratio equal to a function of number of blades, helix angle, and radius. For lightly loaded propellers,

$$K(x) = \frac{B\Gamma n}{Vw} = f(B, \phi, x)$$

or alternatively for moderately loaded propellers,

$$K(x) = \frac{B\Gamma n}{(V + w)w} = f(B, \phi, x)$$

Theodorsen uses the latter definition.

Mass coefficient.- A factor which Theodorsen uses extensively in his treatment of propeller theory is the mass coefficient k which is the average value over the propeller disk of the circulation function $K(x)$. The mass coefficient is the ratio of the equivalent mass of air accelerated to the uniform velocity w in unit time to the mass of air which passes through the propeller disk during the same time. For a propeller with a finite number of blades, the equivalent mass of air in a cylindrical element of thickness dr to which is imparted the axial velocity w in one turn is

$$dm = \rho(2\pi r\, dr)K(x)\frac{V + w}{n}$$

By an integration over the disk, the equivalent total mass accelerated to velocity w is

$$m = \rho 2\pi R^2 \frac{V + w}{n} \int_0^{1.0} K(x)x\, dx$$

By definition,

$$\frac{m}{\rho\pi R^2 \frac{V + w}{n}} = k = 2\int_0^{1.0} K(x)x\, dx$$

Theodorsen has used an electrical-analogy method to determine values of both the circulation function and the mass coefficient for a wide variety of propellers.

Electrical analogy.- For dual-rotation propellers with symmetrically loaded front and rear units, there is no net rotation in the slipstream; the wake is composed of two sets of helicoidal surfaces spiraling in opposite directions. The configuration of the wake helices is the same whether the oppositely spiraling surfaces of vorticity are regarded as intersecting each other, or as being reflected from one another. For conditions far downstream in the wake of a single-rotation propeller, the value of $K(x)$ at a specified radius on the helicoidal surface is obviously independent of axial position. This independence of axial position does not hold for the circulation function for dual-rotation propellers. The oppositely spiraled vortex sheets intersect (or reflect) to form a symmetrical pattern moving downstream with the velocity w. The circulation function $K(x, \theta)$ for dual-rotation propellers is a periodic function of axial position, one cycle

being the axial distance between successive intersections. The problems involved in determining mathematically the circulation function for dual-rotation propellers were regarded as insurmountably difficult, and Theodorsen turned to the more expedient method of devising a calculating machine to obtain this function. Theodorsen considered investigation of the flow field about and forces on a rigid helicoid when immersed in a liquid and oscillated axially but discarded this scheme as too dependent upon mechanical perfection. However, the mathematical identity of the flow of an ideal fluid with the flow of an electric current in a field of uniform resistance, when boundary conditions are the same, made possible the experimental solution of this problem by electrical analogy.

In the electrical method the counterpart of the rigid helicoidal surfaces trailing the propeller blades is a geometrically similar model of the wake surfaces made of nonconducting material (celluloid). A photograph of several of the wake models is presented as figure 11. The wake model is immersed in a weak electrolytic solution (tap water) in which an electric current flows in a uniform field parallel to the model axis. In this setup electric current and electrical potential are analogous to the velocity and velocity potential of fluid motion, respectively.

Apparatus.- The two types of measurements made with the electrical method were determination point by point of the radial distribution of the circulation function $K(x)$ and determination of the mass coefficient k.

A diagram of the apparatus used for measuring the value of the circulation function $K(x)$ at points along the radius of the helical surface is shown in figure 12. The arrangement is simply a Wheatstone bridge with the usual galvanometer replaced by earphones, and the power supply is alternating current having a frequency of 1000 cycles per second. The null point is established by adjusting the variable resistance until the signal becomes inaudible. The measurement is very precise. The drop in electrical potential δE across a helicoidal surface can be measured accurately at any radius and compared with the potential drop E in a length of the uniform flow field equivalent to the axial spacing between adjacent sheets. The electrical analogy shows the circulation function to be

$$K(x) = \frac{\delta E}{E}$$

Somewhat similar apparatus (fig. 13) is used for measuring the mass coefficient k which, being an integrated quantity, requires only a single measurement for each model. Two arms of the Wheatstone bridge are known resistances and the other two are the identical tanks of electrolyte. The tank walls are nonconducting, but the top and bottom

are copper plates in contact with the electrolyte. Between the copper plates of one tank is inserted a model of the helicoidal wake coaxially with the tank. The increase in electrical resistance caused by the presence of the wake model is equivalent to the addition of a potential opposing that of the uniform flow and results in a decreased current. Theodorsen gives rigorous proof that the mass coefficient is

$$k = \frac{\Delta I}{\left(\frac{F}{S}\right) I_o}$$

where F and S are the cross-sectional areas of the wake model and tank, respectively, I_o is the current flowing in the unobstructed tank, and ΔI is the change in current due to the presence of the wake model.

The reliability of the electrical-analogy method was verified by a comparison of the experimental results with those obtained by the exact theory (Goldstein) for the known case of a single-rotation propeller having two blades. The comparison is given in figure 14 which presents the mass coefficient plotted against the advance ratio of the wake. The agreement is excellent.

The difference in radial distribution of the circulation function for single-rotation and dual-rotation propellers is illustrated in figure 15 for four-blade propellers operating at an advance ratio of 6.0. The dual-rotation propeller is composed of two units of two blades each, rotating in opposite directions. The value of $K(x)$ is of necessity zero at the blade tip for both propellers and zero at the axis also for the single-rotation propeller, but for the dual-rotation propeller $K(x)$ increases continuously with distance from the tip and reaches a maximum value at the axis of rotation. In order to draw an analogy between the propeller and a wing, the single-rotation-propeller blade behaves in effect as a wing having a span equal to the propeller radius, whereas the dual-rotation-propeller blade acts as the semispan of a wing the full span of which is the propeller diameter. Consider two oppositely rotating blades of an ideal dual-rotation propeller when 180° apart. The bound circulations on the two blades are symmetrical, equal, and are in the same sense; hence there is no concentration of vorticity shed along the axis of rotation as in the case of the single-rotation propeller. If a comparison were made of the radial distribution of thrust for the two propeller types, the thrust-grading curves for both would be zero at the axis and at the tip, but the elemental values of thrust for the dual-rotation propeller would, at all radii, be greater than those for the single-rotation propeller if the same value of wake velocity w is assumed for both cases.

As mentioned in the discussion of the mass coefficient this factor represents the portion of the slipstream flow effectively worked on by

the propeller. A comparison of the mass coefficients for four-blade single-rotation and dual-rotation propellers is shown in figure 16. At values of advance ratio currently in use for cruising operation, $J = 1.5$ to 3.0, the mass coefficient for the dual-rotation propeller is about twice that for the single, and about three times as great at values of advance ratio from 4.0 to 5.0. This comparison shows that for the case selected, for operation at equal values of induced loss the power capacity of a dual-rotation propeller is much greater than that of a single-rotation propeller of equal diameter and solidity.

DISCUSSION

In his book on propeller theory (reference 33) Theodorsen comments that the theory for dual-rotation propellers may be overidealized. The ideal distribution of circulation cannot be obtained in practice by any means known at present, because the theory demands a cyclic change in the circulation function which in turn requires a cyclic change in blade angle. The required cyclic pitch change is different for each radial station and, therefore, cannot be obtained by a simple oscillation of a blade in the hub.

The validity of the electrical analogy, though apparently well verified by comparison with theory for single-rotation propellers, is not completely established for dual-rotation propellers. The radial lines of intersection of the sets of oppositely spiraling vortex sheets represent regions of discontinuity. There is no guarantee that the application of the electrical analogy with celluloid models of dual-propeller wakes faithfully represents the operation of actual dual-rotation air propellers, especially in the practical case in which the dual units operate in tandem rather than in the same plane.

All propeller theory has been developed for operation in an incompressible fluid. The theories apply well in a compressible fluid at subsonic speeds up to those at which the blade sections reach their critical values of Mach number. At higher subsonic speeds some portion of the blade always operates in a region of transonic flow, the blade section lift and drag characteristics undergo rapid changes, and the load distribution calculated for ideal conditions is meaningless. With adequate knowledge of airfoil characteristics at transonic speeds, however, a propeller can be designed to operate with the ideal load distribution for one particular operating condition in the transonic region. The design of an efficient propeller with least induced energy loss for operation at transonic and low supersonic speeds depends only on the availability of airfoil characteristics for the corresponding values of blade-section Mach number. Inasmuch as the propeller wake velocity is only a few percent of the velocity of flight, the induced velocities are entirely subsonic even for transonic and supersonic propellers. The theoretically desirable distribution of circulation along the blade for incompressible flow should hold for transonic and low supersonic flight speeds as well as it does in the low subsonic range.

APPENDIX

SYMBOLS

a	inflow velocity factor ($B = \infty$)
a'	rotational interference velocity factor ($B = \infty$)
B	number of blades
b	blade width (chord)
c_d	section drag coefficient
c_l	section lift coefficient
C_P	power coefficient $\left(P/\rho n^3 D^5\right)$
C_T	thrust coefficient $\left(T/\rho n^2 D^4\right)$
D	propeller diameter
E	electrical potential, volts
F	cross-sectional area of model helicoidal wake projected on a plane normal to axis
H	total pressure
I	electric current, amperes
I_o	electric current in uniform field, amperes
J	advance ratio (V/nD)
$K(x)$	the circulation function $\left(\frac{B\Gamma n}{(V + w)w}\right)$
k	mass coefficient $\left(2\int_0^{1.0} K(x)x\,dx\right)$
L	lift
m	mass flow, slugs per second

n rotational speed, revolutions per second

P power

p static pressure

p_o free-stream static pressure

R propeller tip radius; electrical resistance, ohms

r radius to blade element

S electrolytic-tank cross-sectional area

T thrust

V velocity of advance

W resultant velocity at blade section

w apparent axial velocity of wake helicoidal vortex sheets

w_1 induced velocity normal to helicoidal surface ($w \cos \phi$)

x fraction of propeller-tip radius (r/R)

Γ circulation

$\gamma = \tan^{-1} \frac{c_d}{c_l}$

η efficiency

η_i ideal efficiency, when no drag loss is assumed

η' blade-element efficiency

η_o' blade-element efficiency, when no induced energy loss is assumed

θ angle measured in any plane normal to the axis of rotation, with axis as center

κ Lock's factor $\left(\frac{K(x)}{\cos^2 \phi} \right)$

ρ mass density of air, slugs per cubic foot

σ propeller solidity ($Bb/\pi xD$)

ϕ aerodynamic helix angle

ϕ_o geometric helix angle $\left(\tan^{-1} \frac{J}{\pi x}\right)$

Ω angular velocity, radians per second

REFERENCES

1. Rankine, W. J. M.: On the Mechanical Principles of the Action of Propellers. Trans. Inst. Naval Architects, vol. 6, 1865, pp. 13-39.

2. Froude, W.: On the Elementary Relation between Pitch, Slip, and Propulsive Efficiency. Trans. Inst. Naval Architects, vol. 19, 1878, pp. 47-65.

3. Lanchester, F. W.: Aerodynamics. Constable & Co., Ltd. (London), 1907.

4. Betz, Albert: Schraubenpropeller mit geringstem Energieverlust. Nachrichten d. Kgl. Ges. d. Wissensch. zu Göttingen. Math.-phys. Kl., 1919, pp. 193-217.

5. Goldstein, Sydney: On the Vortex Theory of Screw Propellers. Proc. Roy. Soc. (London), ser. A, vol. 123, no. 792, April 6, 1929, pp. 440-465.

6. Glauert, H.: Airplane Propellers. Airscrew Theory. Vol. IV of Aerodynamic Theory, div. L, ch. I, sec. 4, W. F. Durand, ed., Julius Springer (Berlin), 1935, pp. 179-180.

7. Fage, A., and Collins, H. E.: An Investigation of the Magnitude of the Inflow Velocity of the Air in the Immediate Vicinity of an Airscrew, with a View to an Improvement in the Accuracy of Prediction from Aerofoil Data of the Performance of an Airscrew. R. & M. No. 328, British A.C.A., 1917.

8. Bairstow, Leonard: Applied Aerodynamics. Longmans, Green and Co., 1920.

9. Pistolesi, E.: L'Aerodinamica dell'elica aerea. Estratto dal volume: Sistemi di propulsione per la navigazione aerea e marittima. R. Accad. Sci. Torino, 1942.

10. Glauert, H.: An Aerodynamic Theory of the Airscrew. R. & M. No. 786, British A. R. C., 1922.

11. Helmbold, H. B.: Zur Aerodynamik der Treibschraube. Z.F.M., Jahrg. 15, Heft 13 and 14, 1924, pp. 150-153, and Heft 15 and 16, pp. 170-173.

12. Bienen, Th., and v. Kármán, Th.: Zur Theorie der Luftschrauben. Zeitschr. V.D.I., Bd. 68, Nr. 48, 1924, pp. 1237-1242 and 1315-1318.

13. Kawada, Sandi: Theory of Airscrews. Rep. No. 14 (vol. I, 14) Aero. Res. Inst., Tokyo Imperial Univ., March 1926.

14. Lock, C. N. H., Bateman, H., and Townend, H. C. H.: Experiments to Verify the Independence of the Elements of an Airscrew Blade. R. & M. No. 953, British A.R.C., 1925.

15. Glauert, H.: The Elements of Aerofoil and Airscrew Theory. Cambridge Univ. Press, 1926.

16. Weick, Fred E.: Aircraft Propeller Design. McGraw-Hill Book Co., Inc., 1930.

17. Glauert, H.: Airplane Propellers. Propellers of Highest Efficiency. Vol. IV of Aerodynamic Theory, div. L, ch. VII, sec. 4, W. F. Durand, ed., Julius Springer (Berlin), 1935, p. 263.

18. Lock, C. N. H.: The Application of Goldstein's Theory to the Practical Design of Airscrews. R. & M. No. 1377, British A.R.C., 1932.

19. Lock, C. N. H.: Airscrew Theory. R. & M. No. 1746, British A.R.C., 1936.

20. Lock, C. N. H., and Yeatman, D.: Tables for Use in an Improved Method of Airscrew Strip Theory Calculation. R. & M. No. 1674, British A.R.C., 1935.

21. Crigler, John L., and Talkin, Herbert W.: Charts for Determining Propeller Efficiency. NACA ACR No. L4I29, 1944.

22. Lock, C. N. H.: A Graphical Method of Calculating the Performance of an Airscrew. R. & M. No. 1849, British A.R.C., 1938.

23. Ferri, Antonio: La Determinazione delle velocità indotte da un vortice elicoidale e alcune sue applicazioni allo studio delle eliche. Atti di Guidonia, no. 57-58, 1941.

24. Hartman, Edwin P., and Feldman, Lewis: Aerodynamic Problems in the Design of Efficient Propellers. NACA ACR, Aug. 1942.

25. Biermann, David, and Hartman, Edwin P.: Tests of Two Full-Scale Propellers with Different Pitch Distributions, at Blade Angles up to 60°. NACA Rep. No. 658, 1939.

26. Stack, John: Tests of Airfoils Designed to Delay the Compressibility Burble. NACA Rep. No. 763, 1943.

27. Naiman, Irven: Method of Calculating Performance of Dual-Rotating Propellers from Airfoil Characteristics. NACA ARR No. 3E24, 1943.

28. Collar, A. R.: On the Periodic Effects Experienced by the Blades of a Contra-Rotating Airscrew Pair. R. & M. No. 1995, British A.R.C., 1941.

29. Theodorsen, Theodore: The Theory of Propellers. I - Determination of the Circulation Function and the Mass Coefficient for Dual-Rotating Propellers. NACA Rep. No. 775, 1944.

30. Theodorsen, Theodore: The Theory of Propellers. II - Method for Calculating the Axial Interference Velocity. NACA Rep. No. 776, 1944.

31. Theodorsen, Theodore: The Theory of Propellers. III - The Slip-stream Contraction with Numerical Values for Two-Blade and Four-Blade Propellers. NACA Rep. No. 777, 1944.

32. Theodorsen, Theodore: The Theory of Propellers. IV - Thrust, Energy, and Efficiency Formulas for Single- and Dual-Rotating Propellers with Ideal Circulation Distribution. NACA Rep. No. 778, 1944.

33. Theodorsen, Theodore: Theory of Propellers. McGraw-Hill Book Co., Inc., 1948.

34. Crigler, John L.: Application of Theodorsen's Theory to Propeller Design. NACA RM No. L8F30, 1948.

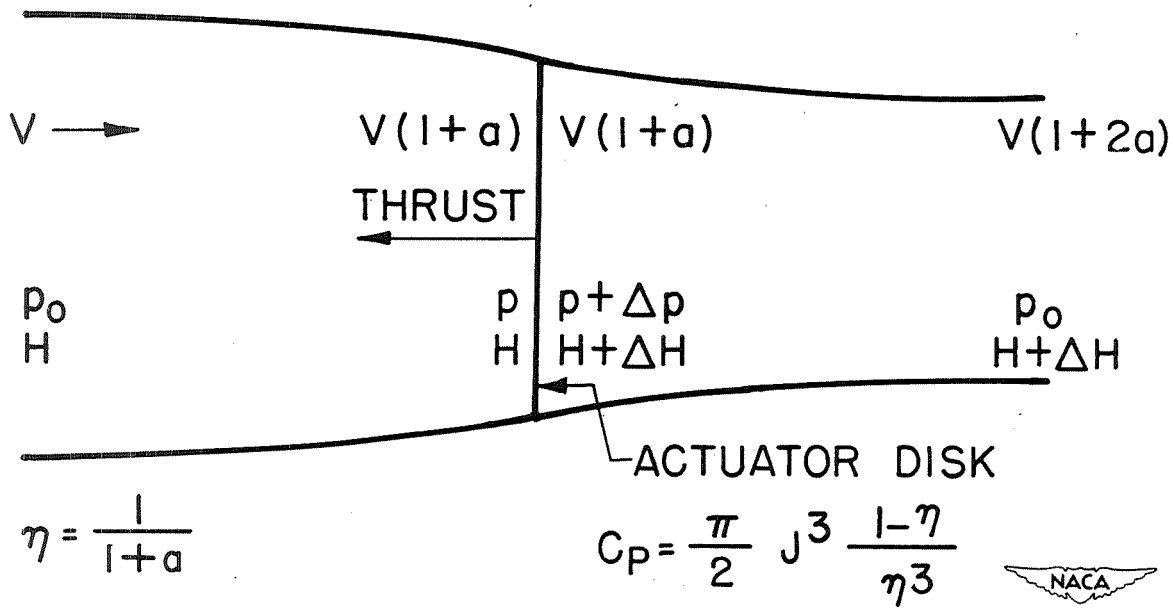

Figure 1.- Simple momentum theory.

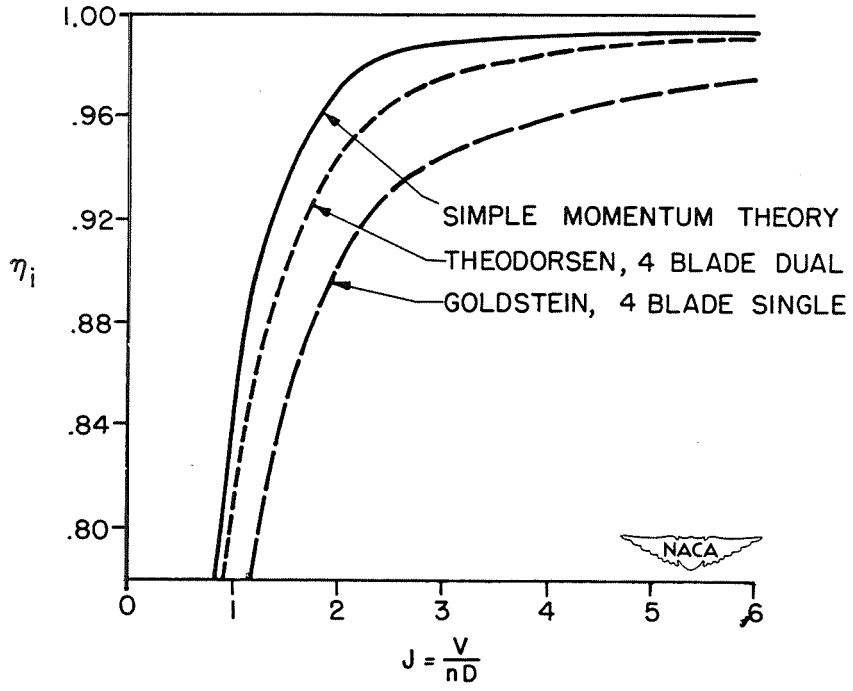

Figure 2.- Ideal efficiency (frictionless propeller); $C_p = 0.4$.

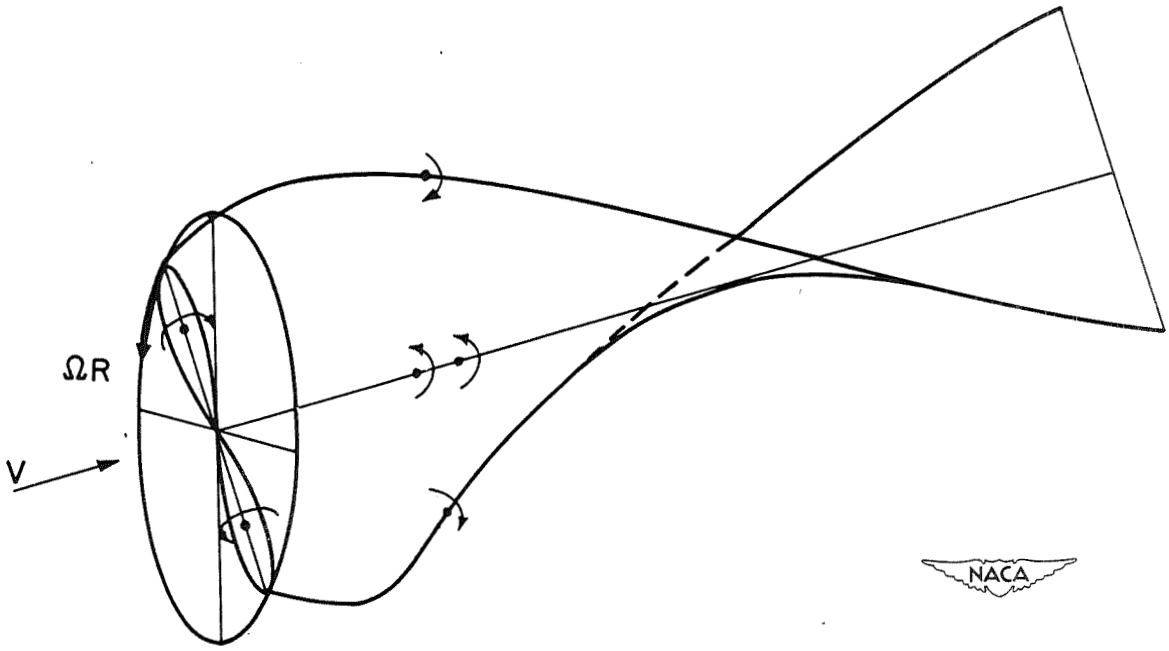

Figure 3.- Basic vortex system for a propeller.

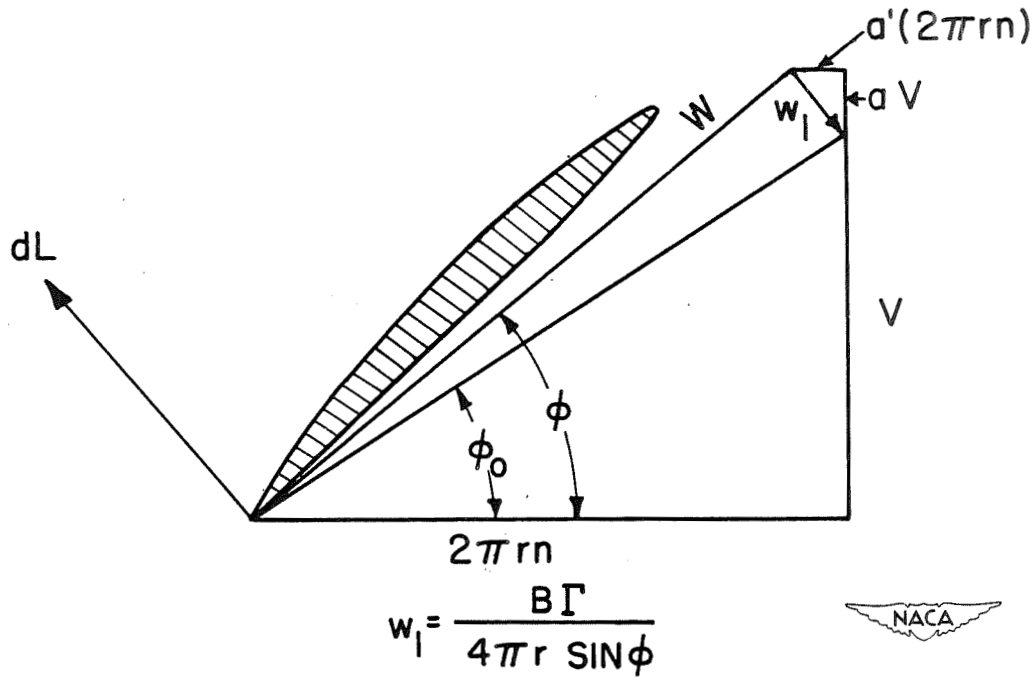

Figure 4.- Vector diagram of vortex blade-element theory; infinite number of blades.

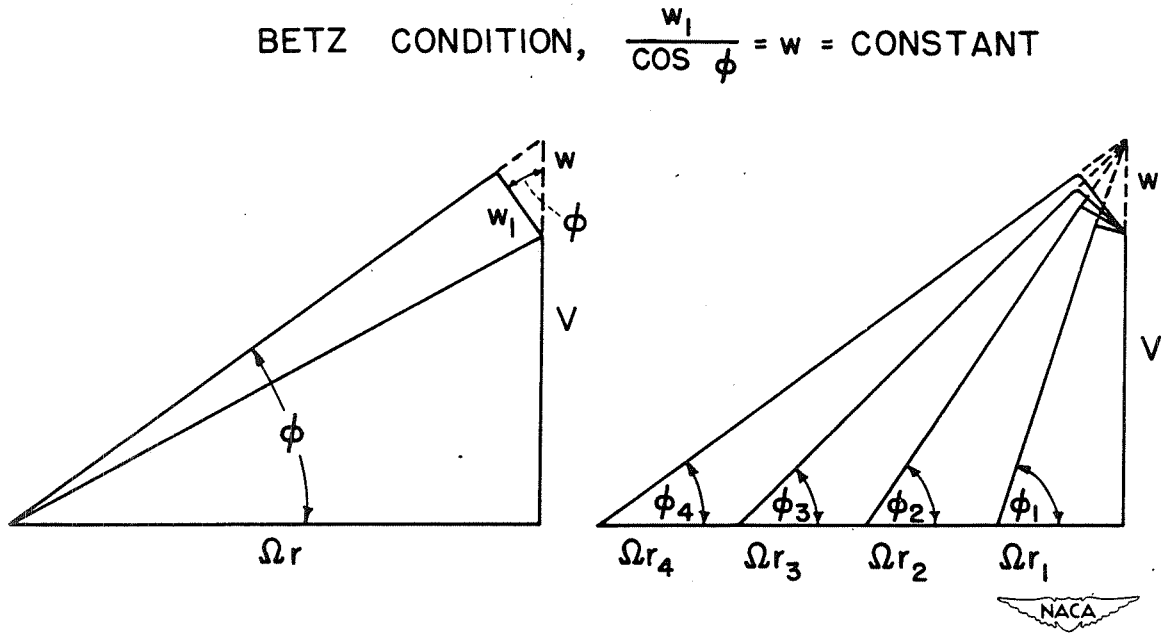

Figure 5.- Radial distribution of induced velocity in rigid helicoidal wake.

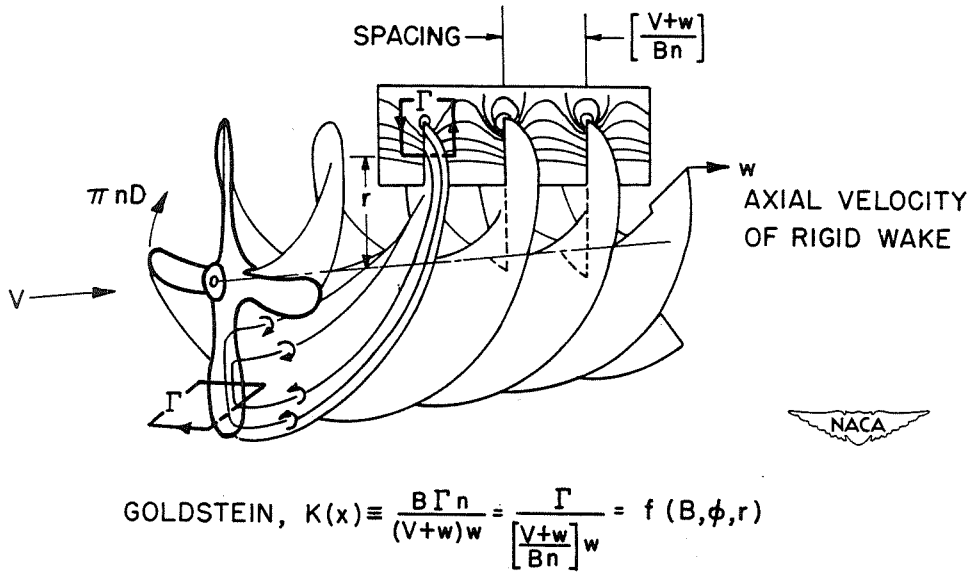

Figure 6.- Circulation function, K(x); finite number of blades.

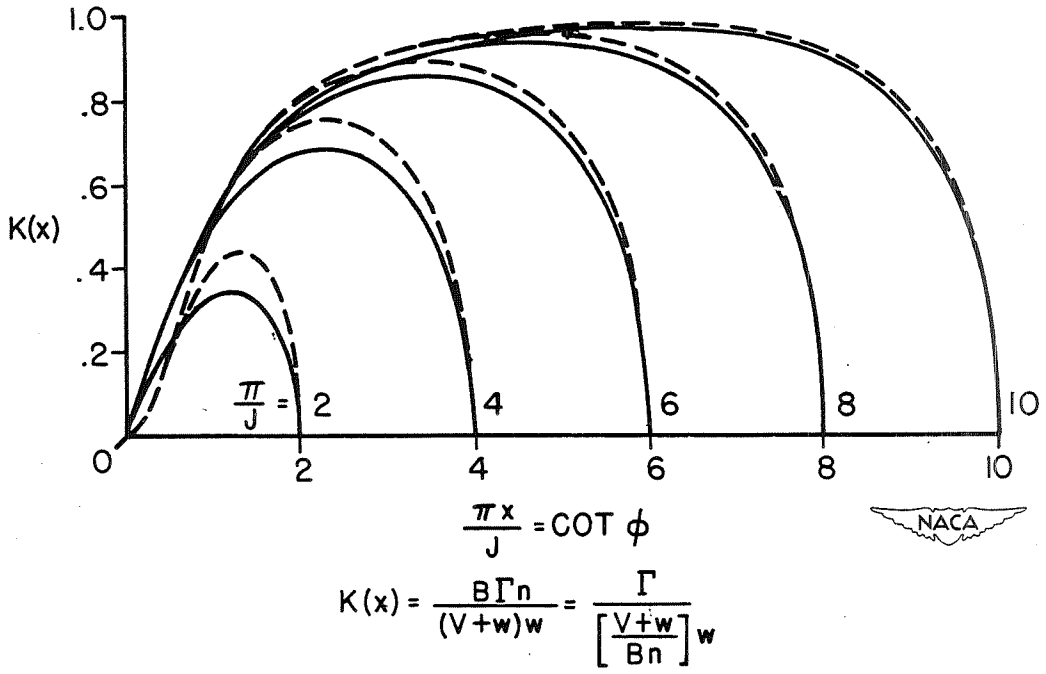

Figure 7.- Goldstein's circulation function; two-blade propeller.

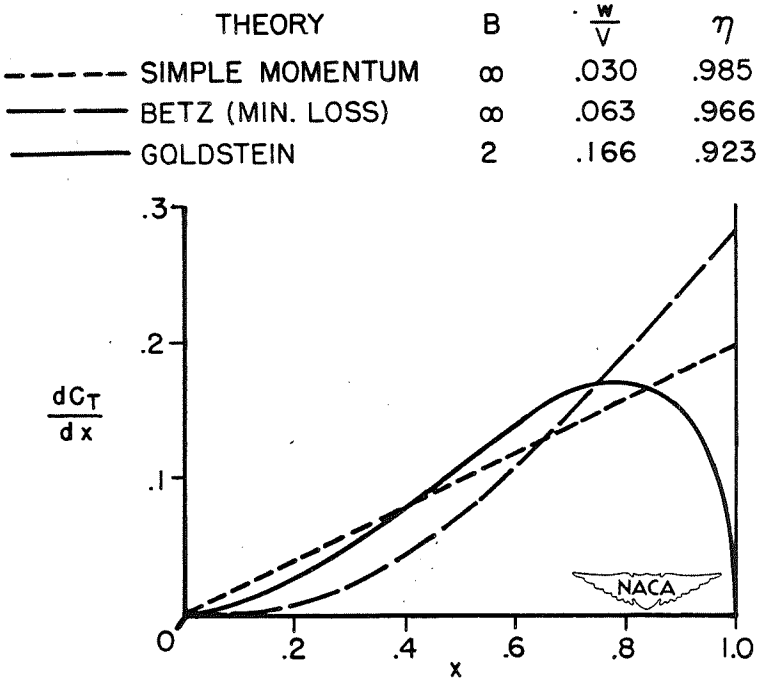

Figure 8.- Comparison of thrust grading curves; $C_p = 0.2$; $J = 2.0$.

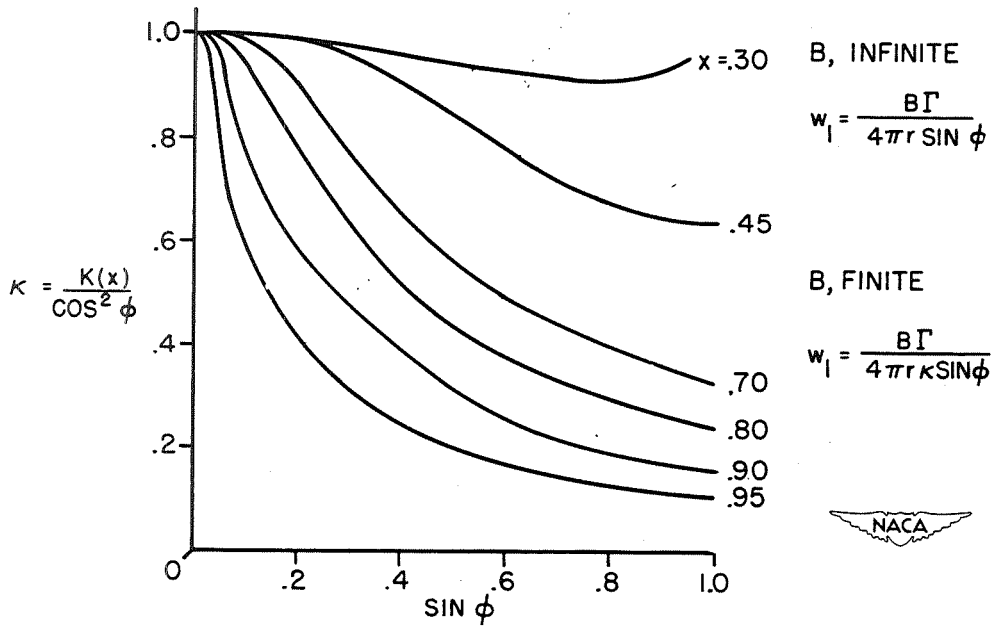

Figure 9.- Lock's presentation of Goldstein circulation function; two-blade propeller.

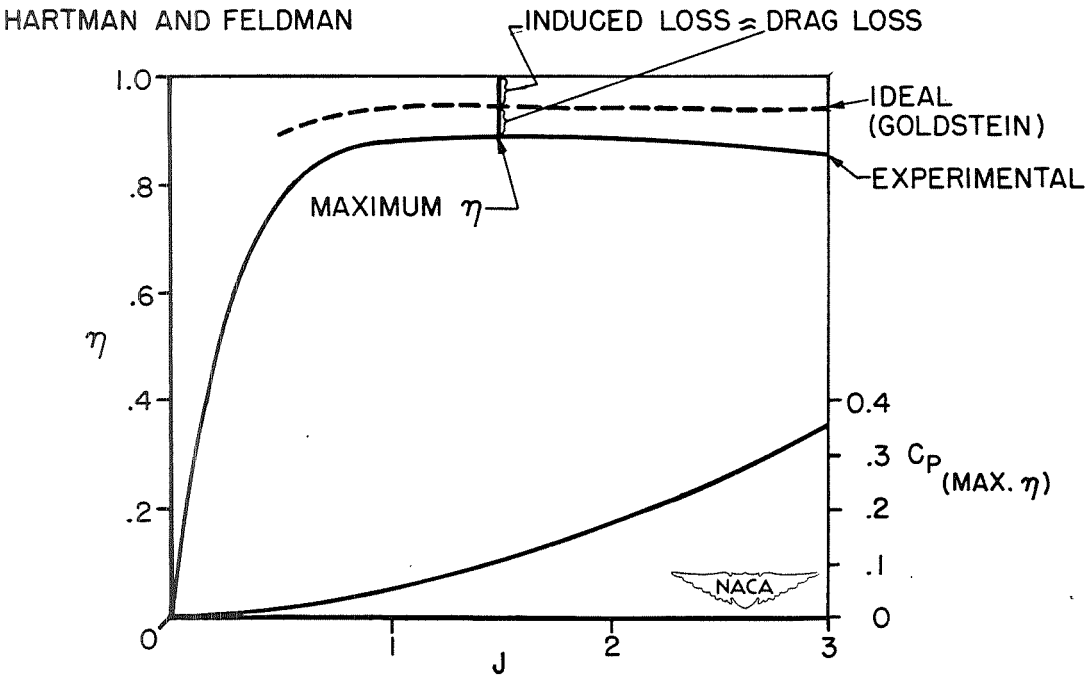

Figure 10.- Envelope efficiency compared with ideal efficiency.

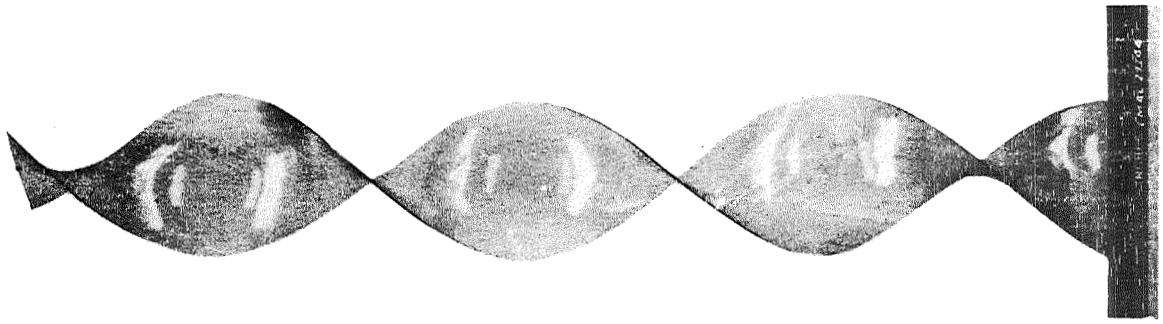

(a) Two-blade single rotation.

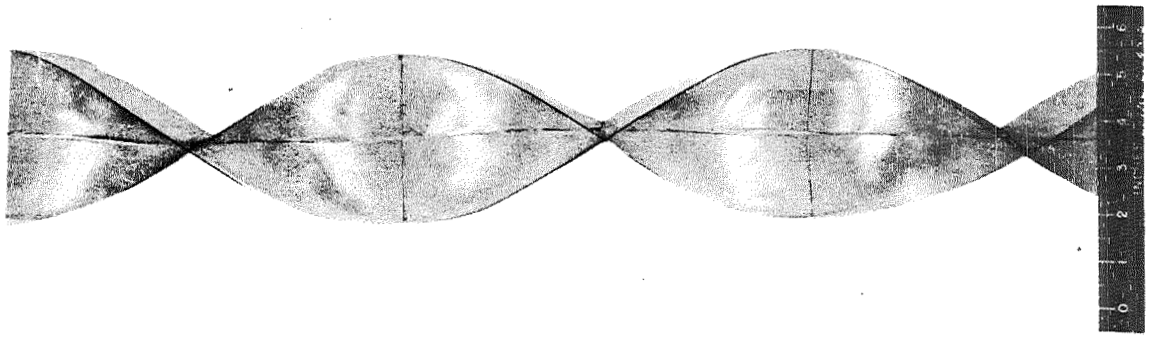

(b) Four-blade dual rotation.

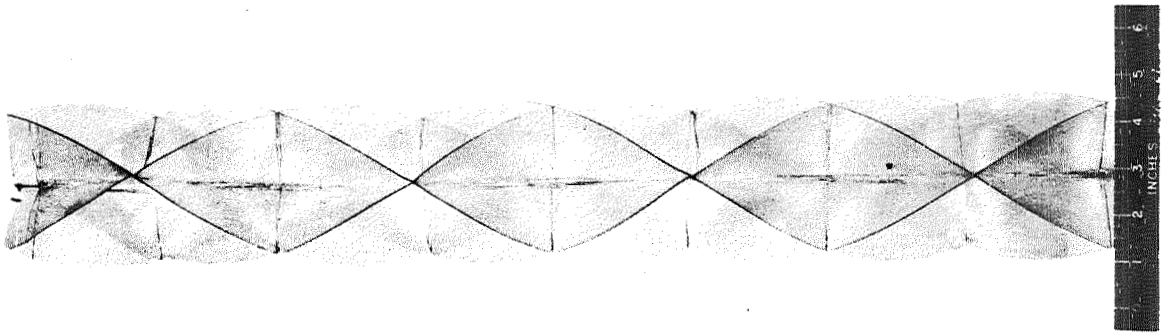

(c) Six-blade dual rotation.

Figure 11.- Typical celluloid wake models used in the electrical-analogy experiments.

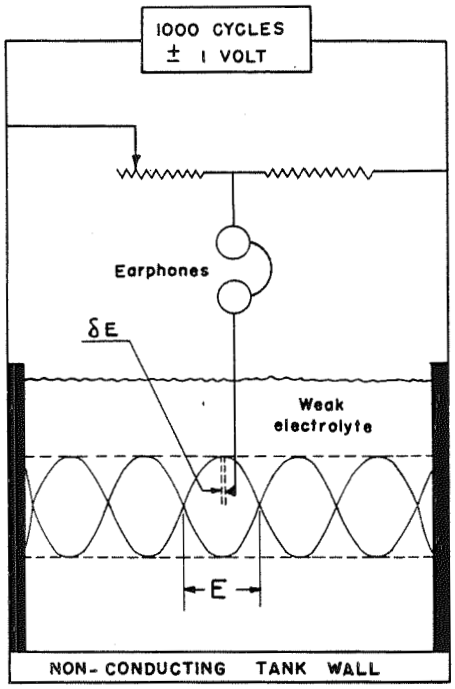

ANALOGY

AERODYNAMIC $\approx$ ELECTRICAL

$$\omega \approx I$$

$$\left[\frac{V+\omega}{Bn}\right] \approx R$$

$$\omega\left[\frac{V+\omega}{Bn}\right] \approx E = IR$$

$$\Gamma \approx \delta E$$

$$K(x) = \frac{\Gamma}{\omega\left[\frac{V+\omega}{Bn}\right]} = \frac{\delta E}{E}$$

NACA

Figure 12.- Schematic diagram of apparatus for measuring the circulation function.

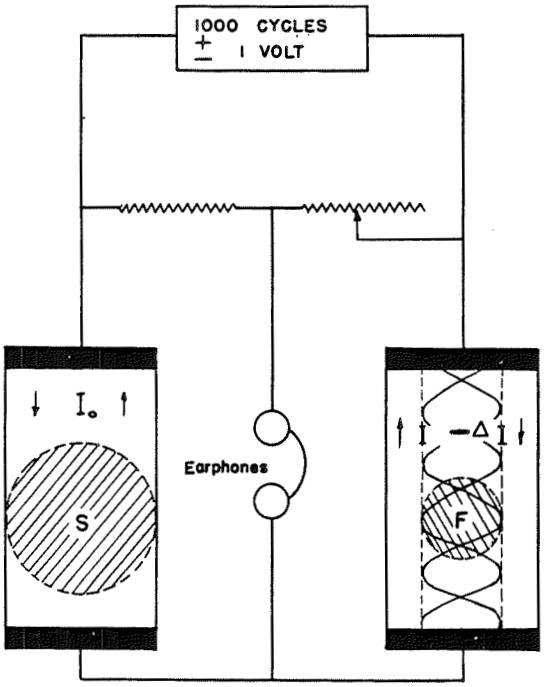

AERODYNAMIC

$$k = 2\int K(x)\, x\, dx$$

$$= \frac{2\int \Gamma x\, dx}{\left[\frac{V+\omega}{Bn}\right]}$$

ELECTRICAL

$$k = \frac{\Delta I}{\left(\frac{F}{S}\right) I_o}$$

NACA

Figure 13.- Schematic diagram of apparatus for measuring the mass coefficient.

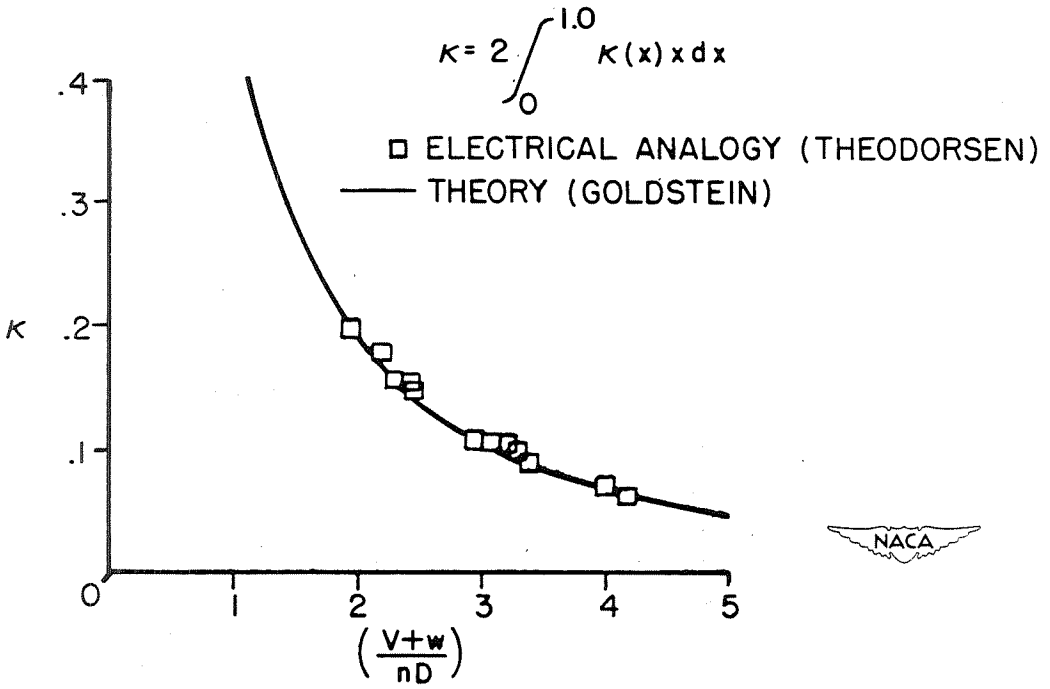

Figure 14.- Electrical-analogy results compared with theory; B = 2.

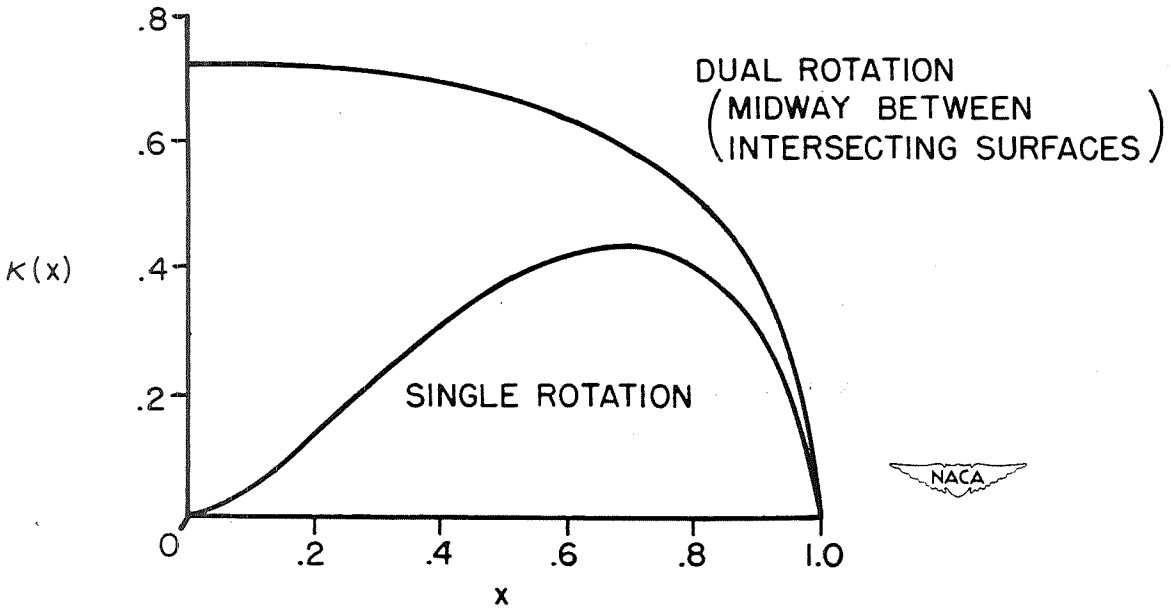

Figure 15.- Radial distribution of load; four-blade propellers; $\frac{V + w}{\pi nD} = 1.89$.